

Strong quantum correlation in a pair hybrid optomechanical cavities

Khadija El Anouz¹, Abderrahim El Allati^{1,2}, and Farhan Saif^{*,4, †}

¹Laboratory of R&D in Engineering Sciences, Faculty of Sciences and Techniques Al-Hoceima, Abdelmalek Essaadi University, Tetouan, Morocco

²The Abdus Salam International Center for Theoretical Physics, Strada Costiera 11, Miramare-Trieste, Italy

^{*}Department of Electronics, Quaid-i-Azam University, 3rd Avenue, Islamabad 45320, Pakistan

⁴Department of Engineering Sciences, University of Electro-Communications, Chofu, Tokyo, Japan

[†]fsaif@yahoo.com

April 3, 2023

Abstract

We show the quantum correlation between two coupled hybrid optomechanical cavities by quantifying the non-classical correlation using Gaussian quantum discord. This involves analyzing and solving Heisenberg Langevin equations to obtain the (12×12) -dimensional covariance matrix of this system. Based on the experimentalist conditions, we simulate quantum correlation of bipartite steady-state with continuous conditions using Gaussian quantum discord. We know that the generation of quantum correlation and its robustness essentially depend on the physical parameters of the system. We provide the stability analysis by means of the Routh–Hurwitz criterion to confirm the choices made during the analysis of quantum discord dynamics.

Keywords: Optomechanical cavities; Gaussian quantum discord, Stability.

1 Introduction

Over few decades, quantum correlations in composite quantum systems leads to develop various fundamental concepts of quantum information and advanced quantum communication techniques [1, 2, 3]. Quantum discord is one of the quantum correlations measures introduced by Ollivier and Zurek [4]. There are many ways to study geometric discord which are Hellinger distance [5], Bures distance [6], trace distance [7], Hilbert-Schmidt distance [8, 9], Gaussian quantum discord [10], and recently local quantum uncertainty [11] and local quantum Fisher information [12]. These of measures have been shown to have a significant impact on the quantification of quantum correlations in deriving their applications as a resource in quantum information processing. Generally, when the quantum discord is expanded to a two-mode Gaussian-like state, the Gaussian quantum discord [10] is a good quantifier of non-classical correlation [13]. The bipartite Gaussian state is correlated if the Gaussian discord is larger than one, while the state is either unentangled or correlated if and only if the Gaussian quantum discord is bounded between zero and one. Interestingly enough, a specific property of quantum correlation is given in the possibility of transmitting information securely between two partners using the quantum teleportation protocol. When implementing a quantum teleportation scheme using a partially or maximized quantum channel, it is necessary to estimate the quality of this protocol by quantifying the fidelity measure, which allows us to assess the similarity between the input and output states during this process [14].

Recently, optomechanical cavities have attracted great attention and created an important addition in quantum technologies because of their experimental realization. These systems interactions of optical and mechanical resonators. Recent experiments involving micro as well as nano-mechanical resonators have proven themselves important in the nano devices [15]. Furthermore, the matter-light joint resonator in optomechanical systems is shown to produce a high-finesse cavity due to the interaction between an array of atoms and a mode of light. A large optomechanical coupling force, which allows the quantum dynamics of moving end-mirror to be controlled via the

intracavity field [16]. Interestingly, in the case where a cavity interacts with a collective density excitation of ultracold atoms, there is a large coupling force [17]. As a result, the combination of cavity quantum electrodynamics. The ultracold gases has enabled a new applications in optomechanical systems [18, 19].

The goal of this paper is to investigate non-classical correlation by means of Gaussian quantum discord. The analysis of the Langevin equations allows to the computation of the covariance matrix of two coupled hybrid optomechanical cavities which made up of two identical Fabry-Pérot cavities of length L with a moving end mirror induced by a single-mode optical field. Each hybrid optomechanical cavity is interacted with a Bose-Einstein Condensates (BEC), with N atoms trapped in an optical lattice potential [20]. Moreover, we suppose that the moving end mirror for each cavity reveals Brownian motion in the absence of coupling with radiation pressure. The obtained covariance matrix is a (12×12) -dimensional matrix and for sake of simplicity we suppose that the cavities are identical. However, in order to investigate quantum correlation by means of Gaussian quantum discord, we shall illustrate from this matrix seven (4×4) submatrices. Indeed, the block covariance matrices, are obtained from the interaction between first intracavity photon-phonon, second intracavity photon-phonon, cavity modes, mechanical resonator modes, BEC-first mechanical mode system, BEC-second mechanical mode system, BEC-first optical mode system. Finally, the last block examines BEC-second mechanical mode system.

The paper is structured as the following: in Sec. 2 we give a detailed description of the proposed model. Sec. 3 includes our calculations used to investigate the Langevin equations and covariance matrix related to the proposed model. In Sec. 4 we gives some preliminaries of Gaussian quantum discord and a discussion of our results. Finally, we conclude our results present and some future directions in Sec. 5.

2 Description of the model

Let's consider a hybrid optomechanical system that allows us to generate quantum correlations in continuous variables between the intracavity optical and mechanical modes. We treat two coupled optomechanical cavities, namely A and B . The optomechanical cavity A (B) is a Fabry-Pérot cavity of length L with a moving end mirror represented by a single-mode optical field of frequency ω_p^A (ω_p^B). Furthermore, the moving end-mirrors exhibit harmonic oscillations denoted by ω_m^i ($i = A, B$), which have Brownian motion in the absence of coupling with radiation pressure. Our main goal is to examine the quantum correlations generated between these cavities. To achieve this goal, we assume that the hybrid optomechanical cavities are interacted with a BEC, with N atoms trapped in an optical lattice potential [21] under the condition of far of resonance. Moreover, the cavities are connected with another via the hopping rate parameter, namely J (See Fig.(1)). Finally, both fixed sides of the hybrid cavities are exposed to the output field of a squeezed light source (SLS).

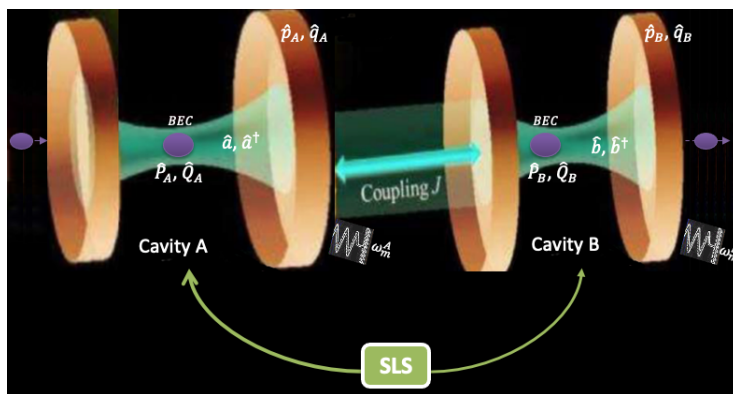


Figure 1: Schematic diagram of the joint optomechanical cavity-cavity system. The cavities are coupled with photon hopping process (PH). Moreover, the fixed sides of the hybrid cavities are exposed to the output field of a squeezed light source (SLS). Each hybrid optomechanical cavity is interacted with a BEC, with N atoms

The total Hamiltonian of the aforementioned model is given as

$$\hat{H} = \hat{H}_1 + \hat{H}_2 + \hat{H}_I + \hat{H}_D, \quad (1)$$

where the Hamiltonian \hat{H}_1 (\hat{H}_2) denotes the atom-optomechanical cavity A (B). The Hamiltonian \hat{H}_I characterizes the interaction between the cavities A and B. While, \hat{H}_D reports the whole effects of dissipation effects including noises and damping related to the system. These Hamiltonians are expressed as follows [22, 23, 24]:

$$\begin{aligned}\hat{H}_1 &= \hat{H}_{f_1}^A + \hat{H}_m^A + \hat{H}_a^A + \hat{H}_{f_2}^A + \hat{H}_{I_1}^A + \hat{H}_{I_1}^A, \\ \hat{H}_2 &= \hat{H}_{f_1}^B + \hat{H}_m^B + \hat{H}_a^B + \hat{H}_{f_2}^B + \hat{H}_{I_1}^B + \hat{H}_{I_1}^B, \\ \hat{H}_I &= J(\hat{b}^\dagger \hat{a} + \hat{a}^\dagger \hat{b}),\end{aligned}\quad (2)$$

where the operators $a(a^\dagger)$ and $b(b^\dagger)$ are the annihilation (creation) operators within cavities A and B, respectively. Various Hamiltonians offered in Eq.(2), namely $\hat{H}_{f_1}^{A(B)}$, $\hat{H}_m^{A(B)}$, $\hat{H}_a^{A(B)}$, $\hat{H}_{f_2}^{A(B)}$, $\hat{H}_{I_1}^{A(B)}$ and $\hat{H}_{I_1}^{A(B)}$ are the Hamiltonians of the field inside cavity A(B), moving-end mirror in cavity A(B), atom, the field arrived from the desexcitation of the atom inside cavity A(B), the coupling between the field and the moving-end mirror and the coupling between the atom and the field Hamiltonians, respectively. They take the following compact form

$$\begin{aligned}\hat{H}_{f_1}^A &= \hbar\Delta_A \hat{a}^\dagger \hat{a}, \\ \hat{H}_{f_1}^B &= \hbar\Delta_B \hat{b}^\dagger \hat{b}, \\ \hat{H}_m^{A(B)} &= \frac{\hbar\omega_m^{A(B)}}{2}(\hat{p}_{A(B)}^2 + \hat{q}_{A(B)}^2), \\ \hat{H}_a^{A(B)} &= \frac{\hbar\Omega_{A(B)}}{2}(\hat{P}_{A(B)}^2 + \hat{Q}_{A(B)}^2), \\ \hat{H}_{f_2}^A &= \frac{\hbar U_0^A N^A}{2} \hat{a}^\dagger \hat{a}, \\ \hat{H}_{f_2}^B &= \frac{\hbar U_0^B N^B}{2} \hat{b}^\dagger \hat{b}, \\ \hat{H}_{I_1}^A &= -\zeta_A \hbar \hat{a}^\dagger \hat{a} \hat{q}_A - i\hbar\eta_A(\hat{a} - \hat{a}^\dagger), \\ \hat{H}_{I_1}^B &= -\zeta_B \hbar \hat{b}^\dagger \hat{b} \hat{q}_B - i\hbar\eta_B(\hat{b} - \hat{b}^\dagger), \\ \hat{H}_{I_2}^A &= \xi_m^A \hbar \hat{a}^\dagger \hat{a} \hat{Q}_A, \\ \hat{H}_{I_2}^B &= \xi_m^B \hbar \hat{b}^\dagger \hat{b} \hat{Q}_B.\end{aligned}\quad (3)$$

Let's note that $\Delta_{A(B)} = \omega_{A(B)} - \omega_p^{A(B)}$ represents the detuning parameter, such that $\omega_{A(B)}$ is the frequency associated to the cavity A(B). Moreover, \hat{p}_i and \hat{q}_i ($i=A,B$) define the dimensionless momentum and position operators for moving end mirror. Moreover, $\omega_m^{A(B)}$ denotes the harmonic oscillations frequency of moving end mirror system. However, $\Omega_{A(B)}$ defines the recoil frequency of an atom due to the change in energy. Indeed, the atom has dimensionless momentum and position operators, namely $\hat{P}_{A(B)}$ and $\hat{Q}_{A(B)}$, respectively. However, $N^{A(B)}$ denotes the bosonic particles number. Furthermore, U_0^i ($i=A,B$) is the vacuum Rabi frequency, while

$$|\eta_{A(B)}| = \sqrt{\frac{W\kappa_{A(B)}}{\hbar\omega_p^{A(B)}}}\quad (4)$$

is the output power, and $\kappa_{A(B)}$ denotes decay rate associated with cavity A(B) and W is the input laser power. The parameter $\zeta_{A(B)}$ describes the coupling strength parameter characterizing the moving end mirror and intra-cavity field subsystems. The coupling parameter, namely ξ_m^i ($i = A, B$) are associated to the coupling frequency of the field with the atom in each cavity. Finally, let us suppose that the joint optomechanical cavities are pumped by two-mode squeezed light sources (SLS), with identical frequencies ω_{SL} . Indeed, the SLS are distinguished by the photon number and the two-photon correlations, namely $N(\omega_k)$ and $C(\omega_k)$. They are defined as [25],

$$\begin{aligned}N(\omega_k) &= \frac{\Lambda_1^2 - \Lambda_2^2}{4} \left[\frac{1}{(\omega_k - \omega_{SL})^2 + \Lambda_2^2} - \frac{1}{(\omega_k - \omega_{SL})^2 + \Lambda_1^2} \right], \\ C(\omega_k) &= \frac{\Lambda_1^2 - \Lambda_2^2}{4} \left[\frac{1}{(\omega_k - \omega_{SL})^2 + \Lambda_2^2} + \frac{1}{(\omega_k - \omega_{SL})^2 + \Lambda_1^2} \right],\end{aligned}\quad (5)$$

where

$$\begin{aligned}\Lambda_1 &= \frac{1}{2}\pi_1 - \pi_2, \\ \Lambda_2 &= \frac{1}{2}\pi_1 + \pi_2,\end{aligned}\quad (6)$$

where π_1 and π_2 denote the damping strength and amplification parameter associated to the squeezed light source. Without loss of generality, the quantities $N(\omega_k)$ and $C(\omega_k)$ can be investigated independently of frequency. The ideal squeezed state implies maximum correlations squeezing to the case $M = \sqrt{N(N+1)}$ (for more details See Refs. [26, 27]).

3 Quantum Langevin equations & Covariance matrix

We focus on the dynamics of the system in the presence of the interaction between the optomechanical cavities. We derive the coupled Langevin equations associated to the operators $\hat{a}, \hat{b}, \hat{p}_{A(B)}, \hat{q}_{A(B)}, \hat{P}_{A(B)}$ and $\hat{Q}_{A(B)}$ using the Hamiltonian defined in Eq.(1). The Langevin equations are obtained as the following form

$$\begin{aligned}
\frac{d\hat{a}}{dt} &= (i\tilde{\Delta}_A + i\zeta_A\hat{q}_A - i\xi_m^A\hat{Q}_A - \kappa_A)\hat{a} - \eta_A + \sqrt{2\kappa_A}\hat{c}_{in} - iJ\hat{b}, \\
\frac{d\hat{b}}{dt} &= (i\tilde{\Delta}'_B + i\zeta_B\hat{q}_B - i\xi_m^B\hat{Q}_B - \kappa_B)\hat{b} - \eta_B + \sqrt{2\kappa_B}\hat{d}_{in} - iJ\hat{a}, \\
\frac{d\hat{p}_A}{dt} &= -\omega_m^A\hat{q}_A + \xi_A\hat{a}^\dagger\hat{a} - \gamma_m^A\hat{p}_A + \hat{I}_A(t), \\
\frac{d\hat{p}_B}{dt} &= -\omega_m^B\hat{q}_B + \xi_B\hat{b}^\dagger\hat{b} - \gamma_m^B\hat{p}_B + \hat{I}_B(t), \\
\frac{d\hat{q}_A}{dt} &= -\omega_m^A\hat{p}_A, \\
\frac{d\hat{q}_B}{dt} &= -\omega_m^B\hat{p}_B, \\
\frac{d\hat{P}_A}{dt} &= \Omega_A\hat{Q}_A + \xi_m^A\hat{a}^\dagger\hat{a} - \gamma_{sm}^A\hat{P}_A + \hat{I}_{1m}^A(t), \\
\frac{d\hat{P}_B}{dt} &= \Omega_B\hat{Q}_B + \xi_m^B\hat{b}^\dagger\hat{b} - \gamma_{sm}^B\hat{P}_B + \hat{I}_{1m}^B(t), \\
\frac{d\hat{Q}_A}{dt} &= -\Omega_A\hat{P}_A - \gamma_{sm}^A\hat{Q}_A + \hat{I}_{2m}^A(t), \\
\frac{d\hat{Q}_B}{dt} &= -\Omega_B\hat{P}_B - \gamma_{sm}^B\hat{Q}_B + \hat{I}_{2m}^B(t),
\end{aligned} \tag{7}$$

where $\tilde{\Delta}_{A(B)} = \Delta_{A(B)} + \frac{U^{A(B)}N^{A(B)}}{2}$, and $\gamma_{m(sm)}^{A(B)}$ are the mechanical energy decays, while $\hat{I}_{A(B)}$ and $\hat{I}_{1m(2m)}^{A(B)}$ are Brownian noise operators [29]. In general, they satisfy the following property

$$\langle I_{A(B)}(t)I_{A(B)}(t') + I_{A(B)}(t')I_{A(B)}(t) \rangle / 2 = \gamma_m^{A(B)}(2\bar{n}_{A(B)} + 1)\delta(t - t'), \tag{8}$$

such that $\bar{n} = (e^{\frac{\hbar\omega_m}{k_B T}} - 1)^{-1}$ denotes the mean vibrational number, where, k_B defines Boltzmann constant, ω_m is the mechanical resonator frequency and T is the temperature of the environment. Moreover, we have used the following properties:

$$[\hat{a}, \hat{a}^\dagger] = \tilde{I}_d, \quad [\hat{b}, \hat{b}^\dagger] = \tilde{I}_d,$$

$$[\hat{q}, \hat{p}] = iI_d, \quad [\hat{Q}, \hat{P}] = iI_d.$$

Finally, the input-output theory is also used via following formulas [30]

$$\begin{aligned}
\hat{a}(t) &= \sqrt{2\kappa_A}\hat{c}_{in}(t) - \kappa_A\hat{a}(t), \\
\hat{b}(t) &= \sqrt{2\kappa_B}\hat{d}_{in}(t) - \kappa_B\hat{b}(t).
\end{aligned}$$

The first and second Langevin equations in (7) clearly show that the optical resonators of modes \hat{a} and \hat{b} are mathematically coupled via the coupling strength, J . Hence, based on the coupled Langevin equations (7), one can straightforwardly illustrate the covariance matrix of the proposed optomechanical system (for more details see Appendix A). In fact, the covariance matrix is has a (12×12) -dimensional matrix. However, in order to investigate

quantum correlation by means of Gaussian quantum discord, we shall illustrate from the whole (8×8) covariance matrix C_v an eight (4×4) submatrices, namely $C_v^{(1)}, C_v^{(2)}, \dots, C_v^{(8)}$ obtained by taking trace operator into account. The first block covariance matrix, namely $C_v^{(1)}$ of the elements kept to the set $\{1, 2, 3, 4\}$ is related to the first intracavity photon-phonon, while the second block covariance matrix, namely $C_v^{(2)}$ of the elements kept to the set $\{5, 6, 7, 8\}$ is attached to the second intracavity photon-phonon. The elements mechanical modes covariance matrix $C_v^{(3)}$ are kept to set $\{1, 2, 5, 6\}$, while the elements cavity modes covariance matrix, namely $C_v^{(4)}$ are kept to set $\{3, 4, 7, 8\}$. On the other hand, the block covariance matrices, namely $C_v^{(5)}$ and $C_v^{(6)}$ of elements kept to the set $\{1, 2, 9, 10\}$ and $\{5, 6, 11, 12\}$ examine the interaction between BEC with the first and second mechanical modes, respectively. Finally, the block covariance matrices, namely $C_v^{(7)}$ and $C_v^{(8)}$ of elements kept to the set $\{3, 4, 9, 10\}$ and $\{7, 8, 11, 12\}$ examine the interaction between BEC with the first and second mechanical modes, respectively.

4 Gaussian quantum discord

Gaussian quantum states represents the core of quantum information through continuous variables. However, the quantum physical statement of quantum information is entanglement. Indeed, the entanglement phenomenon forms a major resource in many tasks in secure information. Interestingly enough, continuous variable entanglement, i.e, entangled Gaussian states have been demonstrated as a worthy measure used to develop several proposals; including cloning, teleportation quantum cryptography, etc. But, entanglement still one kind of the so called quantum correlations. In fact, it have been shown that quantum correlations beyond entanglement can dominate the classical limits in a various proposed cases [28]. Hence, quantum correlations is recognized as a more general way to quantify the separability between quantum systems. In particular, a valuable class of continuous variables correlations measure is Gaussian quantum discord [34]. Quantum discord is investigated as the difference between two expressions of mutual information. The last ones quantumly analogs of classically equivalent information. For a bipartite Gaussian state which is described by its two-mode covariance matrix AB

$$\sigma = \begin{pmatrix} \sigma_1 & \sigma_3 \\ \sigma_3^T & \sigma_2 \end{pmatrix}. \quad (9)$$

Here σ_1 and σ_2 are the covariance matrices attached to the sub-states of system A and B , respectively. Moreover, the matrix σ_3 characterizes the correlations between the two subsystems, namely A and B . Hence, the Gaussian quantum discord is defined as [35, 36]

$$\mathcal{D} = h(\sqrt{b_2}) - h(\sqrt{s^-}) - h(\sqrt{s^+}) + h\left(\frac{\sqrt{b_1 + 2\sqrt{b_1 b_2} + 2I_3}}{1 + 2\sqrt{b_2}}\right), \quad (10)$$

where,

$$\begin{aligned} h(x) &= (x + \frac{1}{2}) \log(x + \frac{1}{2}) - (x - \frac{1}{2}) \log(x - \frac{1}{2}), \\ s^\pm &= \frac{1}{\sqrt{2}} \sqrt{Z \pm \sqrt{Z^2 - 4b_4}}, \\ Z &= b_1 + b_2 + 2I_3, \\ b_1 &= \det \sigma_1, \\ b_2 &= \det \sigma_2, \\ b_3 &= \det \sigma_3, \\ b_4 &= \det \sigma. \end{aligned} \quad (11)$$

where σ_i ($i = 1, 2, 3$) are defined in Eq.(9). The quantities b_j ($j = 1, \dots, 4$) are the so-called symplectic invariants which are still unchanged by all transformations [36], while s^\pm define the symplectic eigenvalues of σ . As mentioned before, we shall investigate eight different block covariant matrices, namely $C_v^{(i)}$. Indeed, the symplectic eigenvalues of partial transpose of each submatrix. It takes the following compact form:

$$s^\pm = \frac{1}{\sqrt{2}} (f_1^i \pm \sqrt{f_1^{i2} - 4f_2^i})^{1/2}, \quad (12)$$

where $f_1^i = \det V_1^i + \det V_2^i - 2 \det V_3^i$ and $f_2^i = \det C_v^i$ ($i = 1, 2, 3$). The matrices V_1^i, V_2^i and V_3^i being the (2×2) block matrices of the whole (4×4) Gaussian states C_v^i as

$$C_v^i = \begin{pmatrix} V_1^i & V_3^i \\ V_3^{iT} & V_2^i \end{pmatrix}. \quad (13)$$

Additionally, for any bipartite Gaussian state defined by its two-mode covariance matrix is entangled when the Gaussian quantum discord in Eq.(10) satisfies $\mathcal{D} > 1$, but this state is unentangled or entangled when $0 \leq \mathcal{D} \leq 1$. The Gaussian quantum discord has been experimentally demonstrated [37, 38]. Within this framework, we are able to quantify the distribution of Gaussian quantum discord between various subsystems of the current study, namely the first intracavity photon-phonon, the second intracavity photon-phonon and the cavity modes subsystems.

4.1 Gaussian quantum discord versus Δ/ω_m for the first and second intracavity photon-phonon system

Before proceeding, it is worth noting that in the plots below, we have chosen some of the parameters regime encoded in the covariance matrix that are close to the topical experiments (See those given in Refs.[39, 40, 41]) which guarantee the stability of the system (See Appendix B). Besides, one can estimate different values of the other parameters, namely the detuning parameter Δ and the mean number of photons, namely n and N , to quantify the Gaussian quantum discord. Moreover, for the sake of simplicity, we assume that both cavities are identical. In this inspiration, we put $\omega_m^A = \omega_m^B = \omega_m, \kappa_A = \kappa_B = \kappa, \gamma_m^A = \gamma_m^B = \gamma_m, T_A = T_B = T, \Delta_A = \Delta_B = \Delta, \Omega_A = \Omega_B = \Omega, \gamma_{sm}^A = \gamma_{sm}^B = \gamma_{sm}$ and $\bar{n}_A = \bar{n}_B = \bar{n}$. Indeed, since the cavities are perfectly identical, then in our numerical results we have obtained the same covariance matrices for the first intracavity photon-phonon and second intracavity photon-phonon. Therefore, in this case, we shall obtain the same behavior for Gaussian quantum discord. However, regardless of the intracavity photon-phonon system, the cavity modes, mechanical resonator modes, BEC-photon and BEC-phonon systems can be also used to quantify the Gaussian quantum discord in our model.

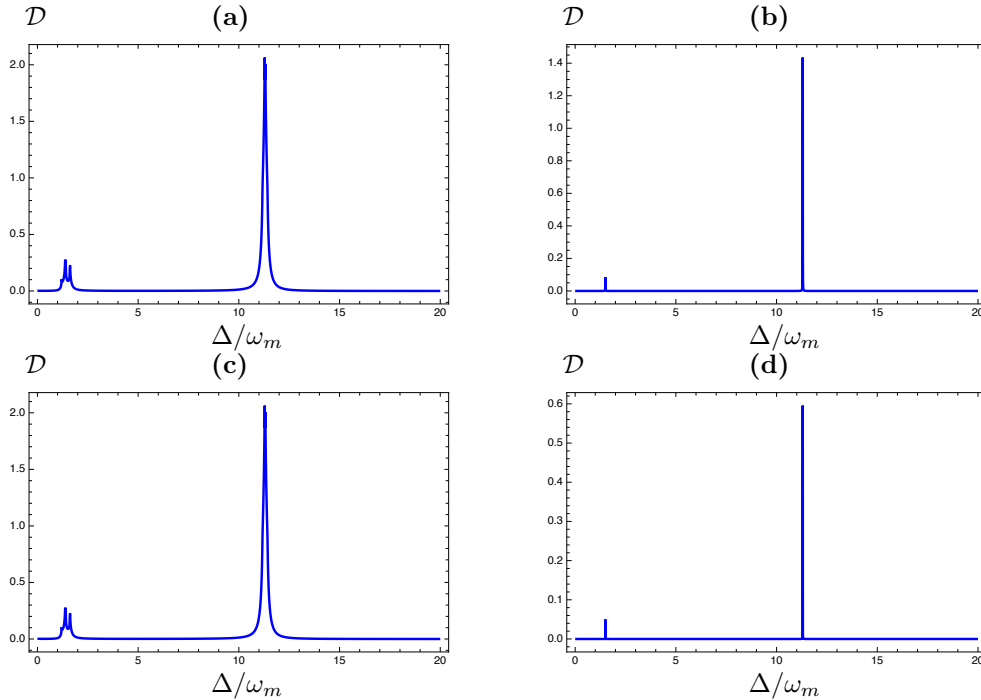


Figure 2: Dynamics of Gaussian quantum discord versus the normalized detuning parameter Δ/ω_m , for the first and second intracavity photon-phonon system. We set, $\kappa = 14 \times 2\pi$ MHz, $\mu^A = \mu^B = S_A = S_B = 8 \times 2\pi$ MHz, $\gamma_m = \gamma_{sm} = 100 \times 2\pi$ MHz, $\Omega = 10 \times 2\pi$. Moreover, (a) $\bar{n} = N = 0, J = 1Hz$, (b) $\bar{n} = 836, N = 0, J = 1Hz$, (c) $\bar{n} = N = 0, J = 0.5Hz$ and (d) $\bar{n} = 14642, N = 0.1, J = 1Hz$.

The plots in Fig. (2) display that the Gaussian quantum discord against the normalized detuning parameter,

namely Δ/ω_m by consideration of various situations. Indeed, in Fig. (2a) we set $\bar{n} = N = 0$ and $J = 1$. The plot shows that the Gaussian quantum discord for the first and second intracavity photon-phonon systems disappears when the normalized detuning parameter vanishes. As Δ/ω_m takes small numbers, the Gaussian quantum discord behaves with small bounds until maximized around $\Delta/\omega_m = 11.5$. A remarkable decreasing appears fast for large numbers of the parameter Δ/ω_m . Indeed, once the normalized detuning parameter increases, the Gaussian discord decreases monotonically until occurring the minimum bounds. On the other hand, the Gaussian discord exceeds one, only when $\Delta/\omega_m = 11.5$ which means that the state is entangled only for this critical value. While, for $\Delta/\omega_m \neq 11.5$ the covariance matrix can be entangled or unentangled since $\mathcal{D} < 1$. In Fig. (2a) we investigate the influence of increasing the parameter \bar{n} . The obtained plot shows the same behaviour but now it is compacted with different upper bound. Indeed, it is clear that the Gaussian quantum discord decreases comparing to Fig. (2a) but the state still always entangled for the critical value of the normalized detuning parameter, namely $\Delta/\omega_m = 11.5$. Now, let examine the impact of small value of the coupling J by keeping always the same initial settings as in Fig. (2a). A similar iour is obtained which means that in this case the parameter J has not a clear effect on the dynamics of Gaussian quantum discord . The plot in Fig. (2c) shows the dynamics of quantum correlation by choosing robust values of \bar{n} and N . It is clear that in this case the state is unentangled for all Δ/ω_m .

4.2 Gaussian quantum discord versus Δ/ω_m for the two mechanical resonator modes system

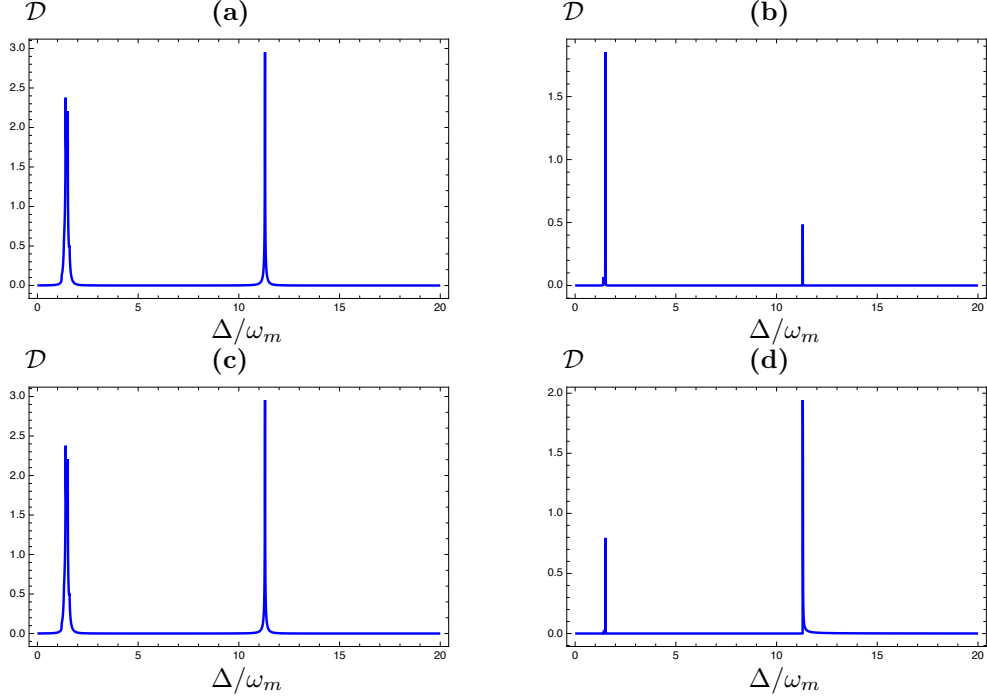


Figure 3: Dynamics of Gaussian quantum discord versus the normalized detuning parameter Δ/ω_m , for the two mechanical resonator modes system. We set, $\kappa = 14 \times 2\pi$ MHz, $\mu^A = \mu^B = S_A = S_B = 8 \times 2\pi$ MHz, $\gamma_m = \gamma_{sm} = 100 \times 2\pi$ MHz, $\Omega = 10 \times 2\pi$. Moreover, (a) $\bar{n} = N = 0$, $J = 1Hz$, (b) $\bar{n} = 836$, $N = 0$, $J = 1Hz$, (c) $\bar{n} = N = 0$, $J = 0.5Hz$ and (d) $\bar{n} = 14642$, $N = 0.1$, $J = 1Hz$.

In Fig.(3), we numerically plot the dynamics of Gaussian quantum discord against the normalized detuning parameter, namely Δ_m/ω_m for the two mechanical resonator modes system. Initially, the Gaussian quantum discord is initially vanished by considering various initial settings of coupled hybrid optomechanical cavities. After a short interval of interaction time t the quantum correlation shows the first peak of $\mathcal{D} > 1$ (correlated cavity-cavity state) except for Fig.(3d) when robust values of the mean numbers of photons \bar{n} and N are considered. For $t > 2$ the Gaussian quantum discord completely vanishes and then increases dramatically with the increasing of the normalized detuning parameter until reached the maximum value around $\Delta/\omega_m \approx 11$. Moreover, it is clear that the

Gaussian quantum discord still non-sensitive to changes in the normalized detuning parameter, for large values of the interaction time parameter, namely t . From Figs.(2) and .(3) one can conclude that the quantum correlations are enhanced using two mechanical resonator modes system.

4.3 Gaussian quantum discord versus Δ/ω_m for the cavity modes system

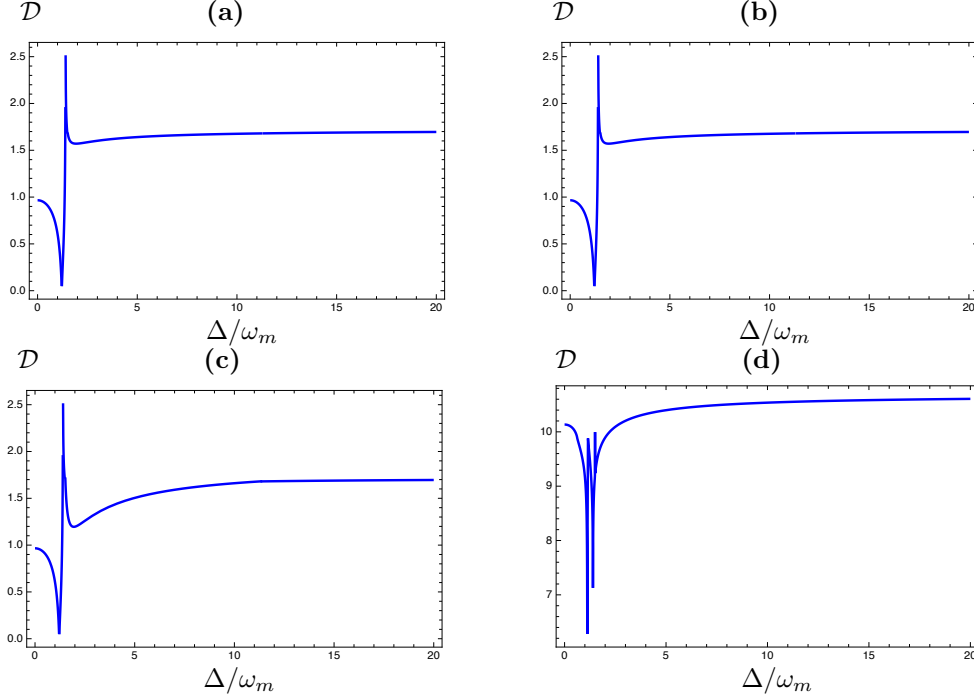


Figure 4: Dynamics of Gaussian quantum discord versus the normalized detuning parameter Δ/ω_m , for the cavity modes system. We set, $\kappa = 14 \times 2\pi$ MHz, $\mu^A = \mu^B = S_A = S_B = 8 \times 2\pi$ MHz, $\gamma_m = \gamma_{sm} = 100 \times 2\pi$ MHz, $\Omega = 10 \times 2\pi$. Moreover, (a) $\bar{n} = N = 0$, $J = 1Hz$, (b) $\bar{n} = 836$, $N = 0$, $J = 1Hz$, (c) $\bar{n} = N = 0$, $J = 0.5Hz$ and (d) $\bar{n} = 14642$, $N = 0.1$, $J = 1Hz$.

Now, let us investigate the quantum correlation of bipartite continuous variable system in terms of the Gaussian quantum discord using intracavity cavity modes system against the normalized detuning, namely Δ/ω_m by varying various parameters encoded in the sub-covariance matrix C_v^4 obtained from Eq.(7). Indeed, from Figs.(4a)-(4c) it is obvious that we recover the same behavior of the Gaussian quantum discord of the cavity modes system for different values of the coupling constant J and the mean number of photons \bar{n} . It is clear that the Gaussian quantum discord for $\Delta/\omega_m = 0$ takes the unity value, while as the normalized detuning parameter increases the quantum discord decreases fast which means that the covariance matrix is either entangled or unentangled since the Gaussian quantum discord indicates an intermediate value between zero and unity. Furthermore, the Gaussian quantum discord increases to owns a maximum pick for small numbers of the normalized detuning parameter, around a critical value, namely $\Delta/\omega_m = 1$. When the normalized detuning parameter is larger than this critical value, the Gaussian quantum discord remains constant even for robust values of Δ/ω_m . In Fig.(4d), we consider the non-zeros of the mean numbers of photons, that is, \bar{n} and N . For this particular case, we clearly observe that the covariance matrix for the cavity modes system is always correlated for all considered values of Δ/ω_m since $\mathcal{D} > 1$. Hence, one can conclude that by controlling various physical parameter of the system (\bar{n} , N and J) we can enhance considerably the amount of quantum correlations by means of Gaussian quantum discord.

4.4 Gaussian quantum discord versus Δ/ω_m for BEC-first mechanical mode system

We devote this subsection to examining the analytical findings of Gaussian quantum discord against the the normalized detuning parameter, namely Δ/ω_m by considering the covariance matrix of the interacted system of BEC

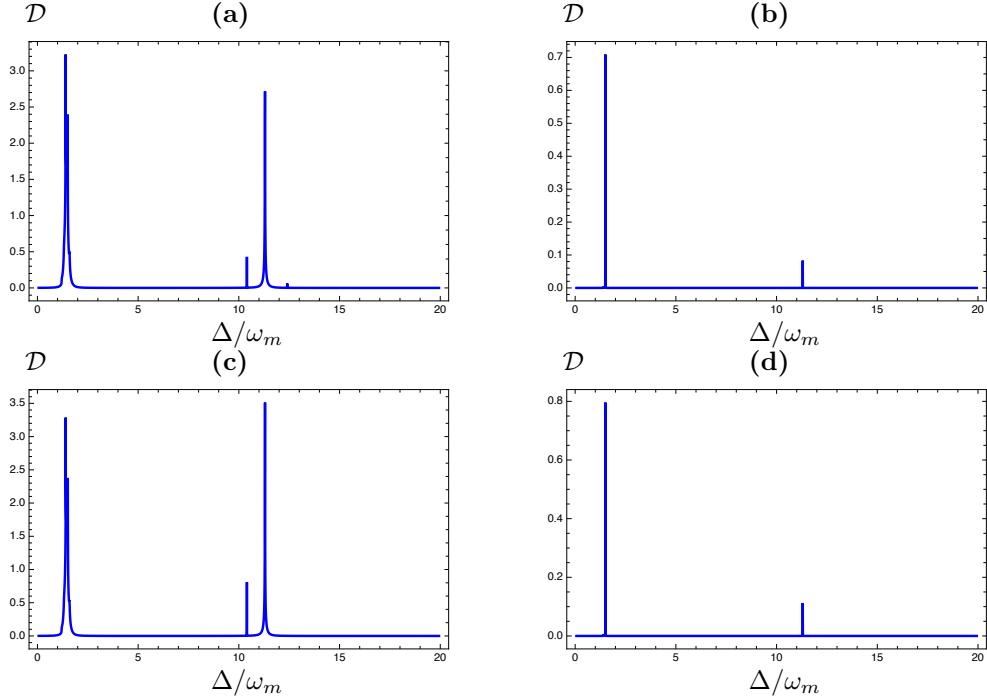


Figure 5: Dynamics of Gaussian quantum discord versus the normalized detuning parameter Δ/ω_m , for BEC-first mechanical mode system. We set, $\kappa = 14 \times 2\pi$ MHz, $\mu^A = \mu^B = S_A = S_B = 8 \times 2\pi$ MHz, $\gamma_m = \gamma_{sm} = 100 \times 2\pi$ MHz, $\Omega = 10 \times 2\pi$. Moreover, (a) $\bar{n} = N = 0$, $J = 1Hz$, (b) $\bar{n} = 836$, $N = 0$, $J = 1Hz$, (c) $\bar{n} = N = 0$, $J = 0.5Hz$ and (d) $\bar{n} = 14642$, $N = 0.1$, $J = 1Hz$.

with the first mechanical mode. Indeed, in Fig.(5) the detuning parameter is used to quantify the non-classical correlation by means of Gaussian quantum discord. Obviously, for Figs.(5a) and (5c), we clearly see that the covariance matrix is entangled for $\Delta/\omega_m = 1.5$ and $\Delta/\omega_m = 11.5$. On the other hand, we assume that $\bar{n} = 836$, $N = 0$, $J = 1Hz$ and $\bar{n} = 14642$, $N = 0.1$, $J = 1Hz$, in Figs.(5b) and (5d), respectively. In this case we clearly see that the Gaussian quantum discord is destroyed from the system since the Gaussian quantum discord indicates never exceeds the unity.

4.5 Gaussian quantum discord versus Δ/ω_m for BEC with second mechanical mode

For the sake of completeness, let's now investigate the quantum correlation of bipartite continuous variable of BEC-second mechanical mode system in terms of the Gaussian quantum discord. When considering the zero-values of the mean number of photons, namely $\bar{n} = N = 0$, we examine the quantum discord \mathcal{D} either by choosing $J = 1Hz$ (Fig.(6a)) or $J = 0.5Hz$ (Fig.(6c)). A similar behaviours are obtained where the sub-covariance matrix $C_v^{(6)}$ is always correlated for the critical values $\Delta/\omega_m = 1.5$ and $\Delta/\omega_m = 11.5$. For the rest of interval, the state is either entangled or separable ($\mathcal{D} < 1$). Furthermore, by raising the mean numbers of photons of the optical modes and SLS, namely \bar{n} and N , respectively (see Figs.(6b) and Fig.(6d)), we observe that the covariance matrix described the interaction between BEC and the mechanical mode of the second optomechanical mode is always correlated since the Gaussian quantum discord indicates the amplitudes larger than unity.

4.6 Gaussian quantum discord versus Δ/ω_m for BEC with first optical mode

Now, let investigate the quantum correlation of bipartite continuous variable system in terms of the Gaussian quantum discord of the intracted BEC and optical inside the first optomechanical cavity against the normalized detuning parameter, namely Δ/ω_m by varying various parameters encoded in the sub-covariance matrices C_v^7 . Indeed, one can see from Figs.(7a) and (7c) that the Gaussian quantum discord is not vanished. As we increase gradually the normalized detuning number, we clearly see that the amount of quantum correlation fluctuate between its maximum and minimum bounds, while it remain constant for some specific interval of Δ/ω_m . Again, by examining

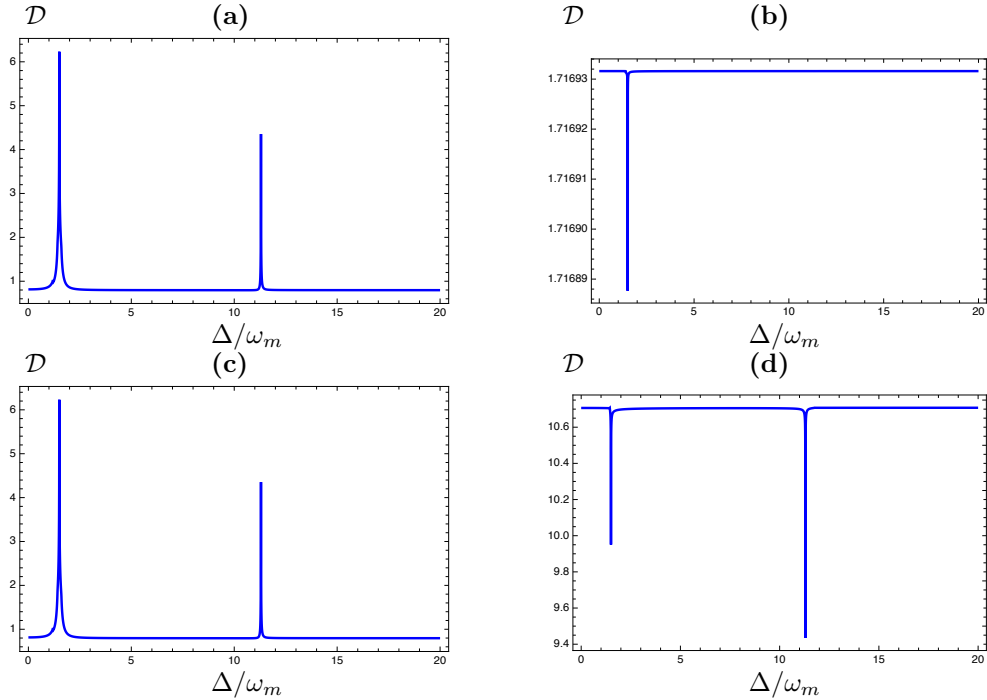


Figure 6: Dynamics of Gaussian quantum discord versus the normalized detuning parameter Δ/ω_m , for BEC-second mechanical mode system. We set, $\kappa = 14 \times 2\pi$ MHz, $\mu^A = \mu^B = S_A = S_B = 8 \times 2\pi$ MHz, $\gamma_m = \gamma_{sm} = 100 \times 2\pi$ MHz, $\Omega = 10 \times 2\pi$. Moreover, (a) $\bar{n} = N = 0$, $J = 1Hz$, (b) $\bar{n} = 836$, $N = 0$, $J = 1Hz$, (c) $\bar{n} = N = 0$, $J = 0.5Hz$ and (d) $\bar{n} = 14642$, $N = 0.1$, $J = 1Hz$.

the large numbers of the means numbers of photons \bar{n} and N in Figs.(7b) and (7d) the behaviours exhibits some few oscillations for small values of the normalized detuning parameter while the Gaussian quantum discord remains constant for the remaining values of Δ/ω_m . Furthermore, for some intervals of detuning parameter, we clearly observe that the covariance matrix is either entangled or unentangled since the Gaussian quantum discord indicates an intermediate value between zero and unity. However for some critical values of Δ/ω_m the state described the BEC-first optical mode system is correlated.

4.7 Gaussian quantum discord versus Δ/ω_m for BEC with second optical mode

Finally, to acquire further insights into quantum correlation of the optomechanical system, we illustrate Fig.(8 the dynamics of quantum correlation by means of Gaussian quantum discord when the BEC interacted with the optical resonator of the second optomechanical cavity. As is clear, we recover the same previous behavior as in Fig.(7) but with different amplitudes. Within this, we clearly see that the covariance matrix of this system, namely C_v^8 is entangled ($\mathcal{D} > 0$) for many critical values of the normalized detuning.

Overall, the peaks appearing in the behaviour of Gaussian quantum discord refer to the transition pattern phenomenon [48]. Indeed, this transition between quantum states occurs through the probabilistic pattern of energy emission or absorption. The transition pattern that emerges from these processes depends on several factors, including the energy difference between the initial and final states, the number and types of particles involved, and the geometry of the system. Importantly, the transition pattern can strongly influence the amount and dynamics of quantum discord. Indeed, the set of transition probabilities that describe the likelihood of the system to transit from one state to another, depends on the number and distribution of resonances in the system. Specifically, it is clear that our systems with higher levels of quantum discord tend to have more complex and nontrivial transition patterns, whereas low levels of quantum discord tend to have more simple and regular transition patterns. Hence, we conclude that the number of resonance transition patterns can affect the quantum discord between subsystems, particularly in systems with a large number of energy levels due to the passage of the BEC system inside the coupled hybrid optomechanical cavities. Close interpretation but with different systems was reported

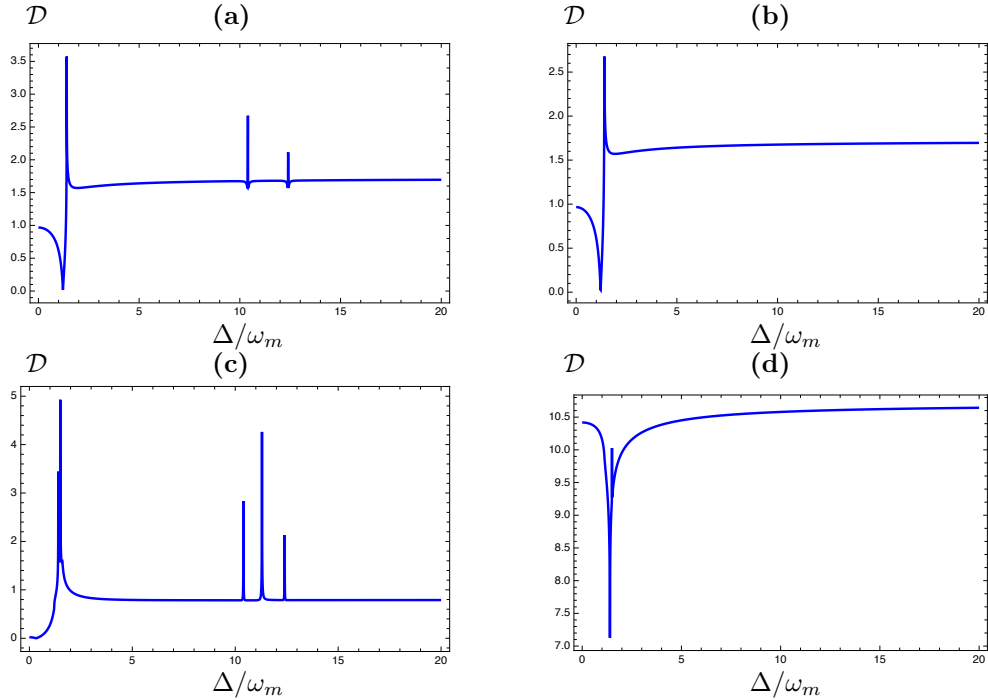


Figure 7: Dynamics of Gaussian quantum discord versus the normalized detuning parameter Δ/ω_m , for BEC-first optical mode system. We set, $\kappa = 14 \times 2\pi$ MHz, $\mu^A = \mu^B = S_A = S_B = 8 \times 2\pi$ MHz, $\gamma_m = \gamma_{sm} = 100 \times 2\pi$ MHz, $\Omega = 10 \times 2\pi$. Moreover, (a) $\bar{n} = N = 0$, $J = 1Hz$, (b) $\bar{n} = 836$, $N = 0$, $J = 1Hz$, (c) $\bar{n} = N = 0$, $J = 0.5Hz$ and (d) $\bar{n} = 14642$, $N = 0.1$, $J = 1Hz$.

in Refs.[49, 50]. Therefore, from the obtained above results we can summarize the necessary conditions used to estimate the quality of correlations between BEC and the coupled hybrid optomechanical cavities. Indeed, we can conclude that one can control various optomechanical parameters. In general, the corresponding covariance submatrices are correlated in particular when the Gaussian quantum discord is plotted with respect to changes in the normalized detuning parameter by keeping various initial settings of mean number of photons, strength coupling between cavities parameters.

5 Conclusion

We presented a simple analysis of the dynamics of an interacted pair of a coupled optomechanical cavities, which we propose to be two Fabry-Pérot cavities of length L with a moving end mirror. Moreover, we have supposed that both cavities are pumped by two-mode squeezed light sources. After exactly solving the set of Langevin equations of the joint optomechanical systems, where each hybrid cavity is interacted with a BEC, we have investigated the quantum correlation. Indeed, we have examined the Gaussian quantum discord between various subsystems of the whole (12×12) covariance matrix, namely the first intracavity photon-phonon, second intracavity photon-phonon, cavity modes, mechanical resonator modes, BEC-first mechanical mode, BEC-second mechanical mode, BEC-first optical mode and BEC-second mechanical mode subsystems. We have concluded that all the Gaussian quantum discord quantifiers of the first and second intracavity photon-phonon oscillate similarly between their upper and lower bounds since we have supposed that both optomechanical cavities are identical. We have found that the obtained covariance matrices are entangled for particular initial settings and for some specific intervals of the normalized detuning parameter. By making a comparative study between the Gaussian quantum discord of the covariance matrices representing the interaction between the pair hybrid optomechanical cavities and BEC, we have obtained some interesting outcomes. In general, we have gained an entangled covariance matrix related to the cavity modes, BEC-first mechanical mode, BEC-second mechanical mode, BEC-first optical mode and BEC-second mechanical mode subsystems while the Gaussian quantum discord for the mechanical modes, first and second intracavity photon-phonon subsystems can be entangled or unentangled since this measure of quantum correlation is lower than one. Indeed, we have concluded that the generation of quantum correlation and its robustness depend

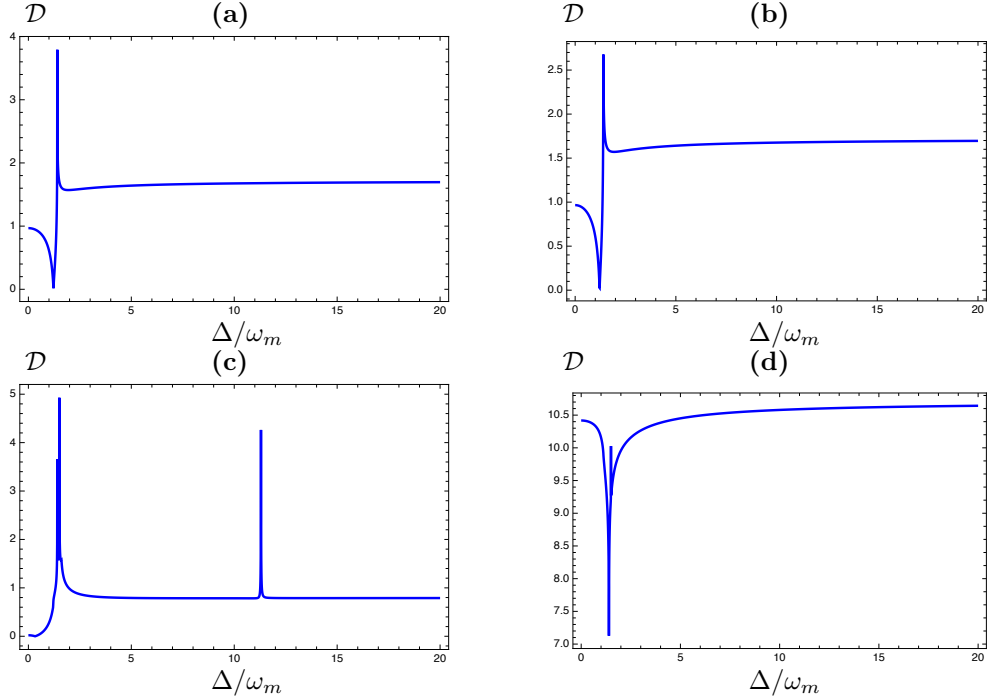


Figure 8: Dynamics of Gaussian quantum discord versus the normalized detuning parameter Δ/ω_m , for BEC-second optical mode system. We set, $\kappa = 14 \times 2\pi$ MHz, $\mu^A = \mu^B = S_A = S_B = 8 \times 2\pi$ MHz, $\gamma_m = \gamma_{sm} = 100 \times 2\pi$ MHz, $\Omega = 10 \times 2\pi$. Moreover, (a) $\bar{n} = N = 0$, $J = 1Hz$, (b) $\bar{n} = 836$, $N = 0$, $J = 1Hz$, (c) $\bar{n} = N = 0$, $J = 0.5Hz$ and (d) $\bar{n} = 14642$, $N = 0.1$, $J = 1Hz$.

basically on the physical parameters of the optomechanical system.

In summary, it is possible to prepare an entangled covariance matrix from the interaction between an interacted two-optomechanical system and BEC, with N atoms trapped in an optical lattice potential. These results can be utilized analytically and experimentally in many areas of quantum information theory and secure communication. Our future perspective will concern other optomechanical systems in order to extend the dimension of the present work. Moreover, it will be motivated for us to investigate other kinds of quantum correlation measures to use them as a good resource in the quantum teleportation protocol and many other applications in quantum information theory.

Appendix A

Here, we give an exhaustive description necessary to compute the whole (12×12) covariance matrix as indicated at the end of section 3. To do this, let first solve the coupled Langevin equations of motion (7). In fact, let's focus our attention on the linearization approach to solve these equations [31]. It consists of assuming that the operators can be amended by small fluctuation from their steady state solutions, namely $\hat{a} = \alpha_s + \delta\hat{a}$, $\hat{b} = \beta_s + \delta\hat{b}$, $\hat{p}_{A(B)} = p_{as(bs)} + \delta\hat{p}_{A(B)}$, $\hat{q}_{A(B)} = q_{as(bs)} + \delta\hat{q}_{A(B)}$. Based on this and conserving only the linear terms, one can obtain the

following coupled equations of motion for the fluctuation parts:

$$\begin{aligned}
\frac{d\hat{\delta}q_A}{dt} &= \omega_m^A \hat{\delta}p_A, \\
\frac{d\hat{\delta}q_B}{dt} &= \omega_m^B \hat{\delta}p_B, \\
\frac{d\hat{\delta}p_A}{dt} &= -\omega_m^A \hat{\delta}q_A - \gamma_m^A \hat{\delta}p_A + \mu_A \hat{\delta}X_A + \hat{I}_A, \\
\frac{d\hat{\delta}p_B}{dt} &= -\omega_m^B \hat{\delta}q_B - \gamma_m^B \hat{\delta}p_B + \mu_B \hat{\delta}X_B + \hat{I}_B, \\
\frac{d\hat{\delta}X_A}{dt} &= -\kappa_A \hat{\delta}X_A + \Delta_A \hat{\delta}Y_A + \sqrt{2\kappa_A} \hat{\delta}X_{in}^A - i \frac{J}{\sqrt{2}} (\beta_s - \beta_s^*) + J \hat{\delta}Y_B, \\
\frac{d\hat{\delta}X_B}{dt} &= -\kappa_B \hat{\delta}X_B + \Delta_B \hat{\delta}Y_B + \sqrt{2\kappa_B} \hat{\delta}X_{in}^B - i \frac{J}{\sqrt{2}} (\alpha_s - \alpha_s^*) + J \hat{\delta}Y_A, \\
\frac{d\hat{\delta}Y_A}{dt} &= -\kappa_A \hat{\delta}Y_A + \Delta_A \hat{\delta}X_A + \sqrt{2\kappa_A} \hat{\delta}Y_{in}^A + S_A \hat{\delta}q_A - J(\beta_s + \beta_s^*) - J \hat{\delta}X_B, \\
\frac{d\hat{\delta}Y_B}{dt} &= -\kappa_B \hat{\delta}Y_B + \Delta_B \hat{\delta}X_B + \sqrt{2\kappa_B} \hat{\delta}Y_{in}^B + S_B \hat{\delta}q_B - J(\alpha_s + \alpha_s^*) - J \hat{\delta}X_A, \\
\frac{d\hat{\delta}Q_A}{dt} &= -\Omega_A \hat{\delta}P_A - \gamma_{sm}^A \hat{\delta}Q_A + \hat{I}_{2m}^A, \\
\frac{d\hat{\delta}Q_B}{dt} &= -\Omega_B \hat{\delta}P_B - \gamma_{sm}^B \hat{\delta}Q_B + \hat{I}_{2m}^B, \\
\frac{d\hat{\delta}P_A}{dt} &= -\nu_A + \Omega_A \hat{\delta}Q_A + \mu_A \hat{\delta}X_A - \gamma_{sm}^A \hat{\delta}P_A + \hat{I}_{1m}^A, \\
\frac{d\hat{\delta}P_B}{dt} &= -\nu_B + \Omega_B \hat{\delta}Q_B + \mu_B \hat{\delta}X_B - \gamma_{sm}^B \hat{\delta}P_B + \hat{I}_{1m}^B.
\end{aligned} \tag{14}$$

Here $\mu_{A(B)} = \sqrt{2}J\alpha_s(\beta_s)$ denotes the effective optomechanical coupling parameter, whereas, α_s and β_s are real, while $\nu_{A(B)} = \xi_m^A |\alpha_s(\beta_s)|^2 - (\frac{\Omega_{A(B)}^2}{\gamma_{sm}^{A(B)}} + \gamma_{sm}^{A(B)})$ and $S_{A(B)} = 2\sqrt{2}\xi_{A(B)}\alpha_s(\beta_s)$. In addition, we took into account the following quadratures as well as input quadrature noise operators:

$$\begin{aligned}
\hat{\delta}X_{A(B)} &= \frac{\delta\hat{a}_{A(B)} + \delta\hat{a}_{A(B)}^\dagger}{\sqrt{2}}, \\
\hat{\delta}Y_{A(B)} &= \frac{\delta\hat{a}_{A(B)} - \delta\hat{a}_{A(B)}^\dagger}{i\sqrt{2}}, \\
\hat{\delta}X_{A(B)}^{in} &= \frac{\delta\hat{a}_{A(B)}^{in} + \delta\hat{a}_{A(B)}^{\dagger in}}{\sqrt{2}}, \\
\hat{\delta}Y_{A(B)}^{in} &= \frac{\delta\hat{a}_{A(B)}^{in} - \delta\hat{a}_{A(B)}^{\dagger in}}{i\sqrt{2}}.
\end{aligned} \tag{15}$$

It is obvious that linearized Langevin equations appeared in Eq.(14) can be reconstruct in the convenient form:

$$\dot{R}(t) = DR(t) + \mathcal{O}(t), \tag{16}$$

where $\mathcal{O}(t)$ denotes the noise vector. It is defined as

$$\mathcal{O}(t) = (0, \sqrt{2\gamma_m^A} \hat{\delta}b_{in}(t), \sqrt{2\kappa_A} \hat{\delta}X_{in}^A(t), \sqrt{2\kappa_A} \hat{\delta}Y_{in}^A(t), 0, \sqrt{2\gamma_B} \hat{\delta}c_{in}(t), \sqrt{2\kappa_B} \hat{\delta}X_{in}^B(t), \sqrt{2\kappa_B} \hat{\delta}Y_{in}^B(t))^T. \tag{17}$$

Moreover, the matrix D in Eq.(16) denotes the drift matrix. Indeed, by keeping all the operators in Eq.(14) except the last four equations since the atom is considered as an auxiliary system (environment) used to connect both cavities. Hence, the drift matrix D is expressed as the following matrix form

$$D = \begin{pmatrix} D_1 & D_2 \\ D_3 & D_4 \end{pmatrix}. \quad (18)$$

where

$$\begin{aligned} D_1 &= \begin{pmatrix} 0 & \omega_m^A & 0 & 0 & 0 & 0 \\ -\omega_m^A & -\gamma_m^A & \mu_A & 0 & 0 & 0 \\ 0 & 0 & -\kappa_A & \Delta_A & 0 & 0 \\ S_A & 0 & \Delta_A & -\kappa_A & 0 & 0 \\ 0 & 0 & 0 & 0 & 0 & \omega_m^B \\ 0 & 0 & 0 & 0 & 0 & -\omega_m^B \end{pmatrix}, & D_2 &= \begin{pmatrix} 0 & 0 & 0 & 0 & 0 & 0 \\ 0 & 0 & 0 & 0 & 0 & 0 \\ 0 & J & 0 & 0 & 0 & 0 \\ -J & 0 & 0 & 0 & 0 & 0 \\ 0 & 0 & 0 & 0 & 0 & 0 \\ -\gamma_m^B & \mu_B & 0 & 0 & 0 & 0 \end{pmatrix} \\ D_3 &= \begin{pmatrix} 0 & 0 & 0 & J & 0 & 0 \\ 0 & 0 & -J & 0 & S_B & 0 \\ 0 & 0 & 0 & 0 & 0 & 0 \\ 0 & 0 & \mu^A & 0 & 0 & 0 \\ 0 & 0 & 0 & 0 & 0 & 0 \\ 0 & 0 & 0 & 0 & 0 & 0 \end{pmatrix}, & D_4 &= \begin{pmatrix} -\kappa_B & \Delta_B & 0 & 0 & 0 & 0 \\ \Delta_B & -\kappa_B & 0 & 0 & 0 & 0 \\ 0 & 0 & -\gamma_{sm}^A & \Omega^A & 0 & 0 \\ 0 & 0 & \Omega^A & -\gamma_{sm}^A & 0 & 0 \\ 0 & 0 & 0 & 0 & -\gamma_{sm}^B & -\Omega^B \\ \mu^B & 0 & 0 & 0 & \Omega^B & -\gamma_{sm}^B \end{pmatrix} \end{aligned} \quad (19)$$

The interaction between the optical and mechanical resonators is characterized by a bipartite state with continuous variables. Let us examine the steady covariance matrix, namely C_v via solving the following Lyapunov equation

$$DC_v + C_v D^T = -F, \quad (20)$$

where F is diffusion matrix, is obtained by the noise correlation functions and by using Eq.(8). The diffusion matrix is obtained as

$$F = \begin{pmatrix} F_1 & F_2 \\ F_3 & F_4 \end{pmatrix}. \quad (21)$$

where

$$\begin{aligned} F_1 &= \begin{pmatrix} 0 & 0 & 0 & 0 & 0 & 0 \\ 0 & \gamma_m(1+2\bar{n}) & 0 & 0 & 0 & 0 \\ 0 & 0 & \kappa(1+2N) & 0 & 0 & 0 \\ 0 & 0 & 0 & \kappa(1+2N) & 0 & 0 \\ 0 & 0 & 0 & 0 & 0 & 0 \\ 0 & 0 & 0 & 0 & 0 & \gamma_m(1+2\bar{n}) \end{pmatrix}, & F_2 &= \begin{pmatrix} 0 & 0 & 0 & 0 & 0 & 0 \\ 0 & 0 & 0 & 0 & 0 & 0 \\ 2M\kappa & 0 & 0 & 0 & 0 & 0 \\ 0 & -2M\kappa & 0 & 0 & 0 & 0 \\ 0 & 0 & 0 & 0 & 0 & 0 \\ 0 & 0 & 0 & 0 & 0 & 0 \end{pmatrix} \\ F_3 &= \begin{pmatrix} 0 & 0 & 2M\kappa & 0 & 0 & 0 \\ 0 & 0 & 0 & -2M\kappa & 0 & 0 \\ 0 & 0 & 0 & 0 & 0 & 0 \\ 0 & 0 & 0 & 0 & 0 & 0 \\ 0 & 0 & 0 & 0 & 0 & 0 \\ 0 & 0 & 0 & 0 & 0 & 0 \end{pmatrix}, \\ F_4 &= \begin{pmatrix} \kappa(1+2N) & 0 & 0 & 0 & 0 & 0 \\ 0 & \kappa(1+2N) & 0 & 0 & 0 & 0 \\ 0 & 0 & \gamma_{sm}(1+2\bar{n}) & 0 & 0 & 0 \\ 0 & 0 & 0 & \gamma_{sm}(1+2\bar{n}) & 0 & 0 \\ 0 & 0 & 0 & 0 & \gamma_{sm}(1+2\bar{n}) & 0 \\ 0 & 0 & 0 & 0 & 0 & \gamma_{sm}(1+2\bar{n}) \end{pmatrix}. \end{aligned} \quad (22)$$

Now, since the drift and diffusion matrices are well known, one can find the corresponding (12×12) covariance matrix via solving numerically the Lyapunov equation in Eq. (20).

Appendix B: Stability criterion

In this appendix, we show that parameters already chosen during our numerical simulations of quantum discord dynamics guarantees stability of the system. Indeed, we provide the stability analysis by means the Routh–Hurwitz

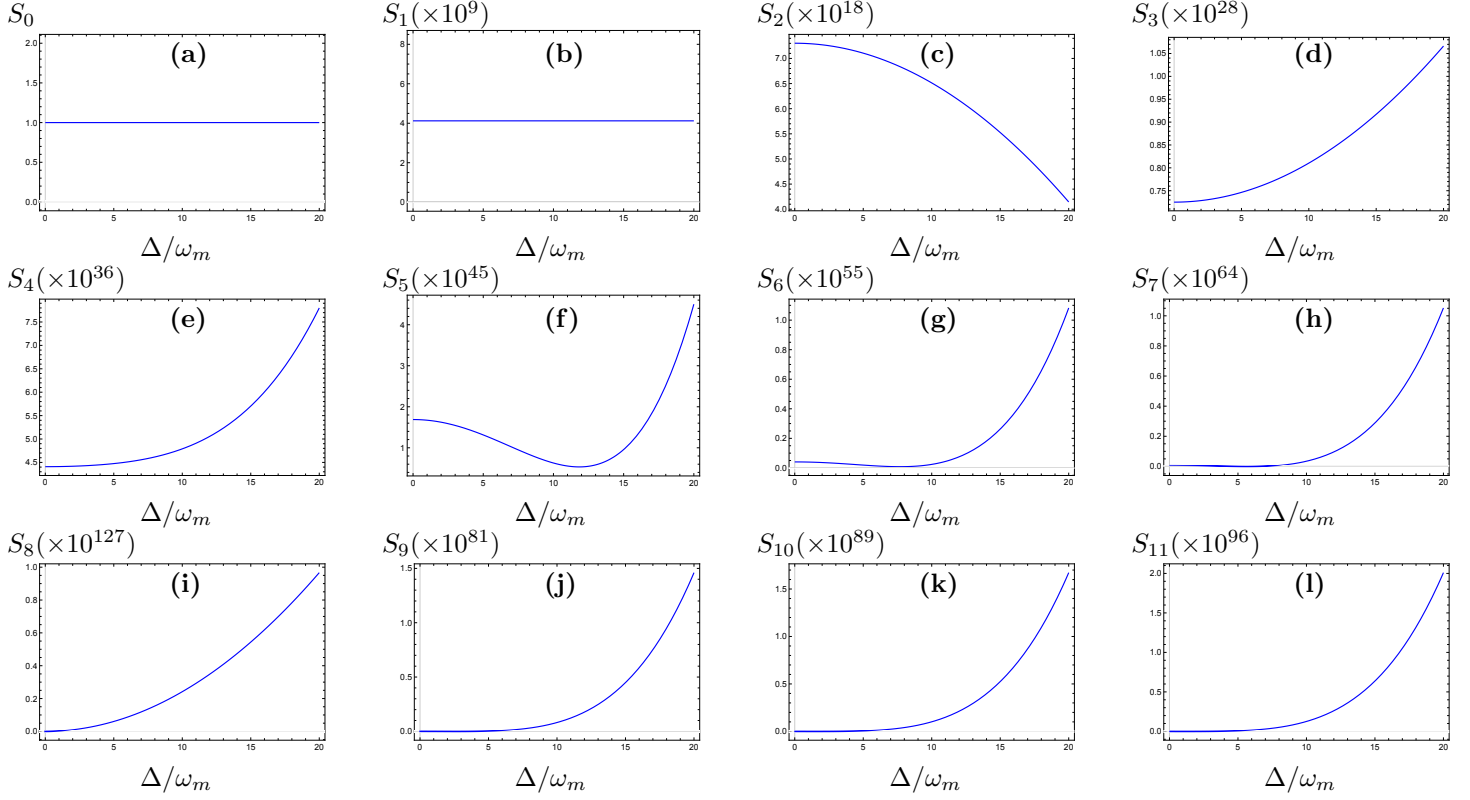


Figure 9: The stability conditions versus the normalized parameter Δ/ω_m where $\kappa = 14 \times 2\pi$ MHz, $\mu^A = \mu^B = S_A = S_B = 8 \times 2\pi$ MHz, $\gamma_m = \gamma_{sm} = 100 \times 2\pi$ MHz, $\Omega = 10 \times 2\pi$ and $J = 1$ Hz.

criterion [46, 47]. In fact the main subject of this criterion is to determine the characters of the solution of the following characteristic equation associated to the drift matrix in Eq.(18) as:

$$S_{11}\lambda^{11} + S_{10}\lambda^{10} + \dots + S_0 = 0. \quad (23)$$

Hence, the Ruth-Hurwitz criterion sets that the system is stable if and only if the characters S_i ($i = 0, \dots, 11$) are positives. In this regard, by imposing the parameters closed to the topical experiments used in our numerical simulations of quantum discord dynamics, we plot in the following figures versus the normalized detuning parameter Δ/ω_m . As it is clear from the figure, the system is completely stable since $S_i > 0$ ($i = 0, \dots, 11$).

Declaration of Interest

The authors declare that they have no conflict of interest.

Data availability statement

No data statement is available.

References

- [1] J. Bub, Quantum Correlations and the Measurement Problem. *Int J. Theor. Phys.* **53**, 3346–3369 (2014).
- [2] S. Köhnke, E. Agudelo, M. Schünemann, O. Schlettwein, W. Vogel, J. Sperling, B. Hage, Quantum Correlations beyond Entanglement and Discord. *Phys. Rev. Lett.* **126**, 170404 (2021).
- [3] M. Navascués, Y. Guryanova, M. Hoban, A. Acín, Almost quantum correlations. *Nat Commun* **6**, 6288 (2015).
- [4] H. Ollivier, W.H. Zurek, Quantum Discord: A Measure of the Quantumness of Correlations. *Phys. Rev. Lett.* **88**, 017901 (2001).
- [5] B. Ye, Z. Zhang, "Quantum correlated coherence and Hellinger distance in the critical systems". *Mod. Phys. Lett. A.* **36**, 2150002 (2021).
- [6] D. Spehner, M. Orszag, "Geometric quantum discord with Bures distance". *New J. Phys.* **15**, 103001 (2013).
- [7] M. Bhatt, "Trace distance: a measure of quantumness". *Int. J. Adv. Res.* **5**, 6 (2017). TRACE DISTANCE: A MEASURE OF QUANTUMNESS.
- [8] G. Adesso and D. Girolami, Gaussian geometric discord, *Int. J. Quan. Inf.* **9**, 1773 (2011).
- [9] S. Seddik, K. El Anouz, A. El Allati, Engineering non-classical correlation and teleportation with Robust fidelity using Jaynes–Cummings model. *Int. J. Geo. Meth. Mod. Phys.* **19**, 2250025 (2022).
- [10] P. Giorda and M. G-A. Paris, Gaussian Quantum Discord, *Phys. Rev. Lett.* **105** (2010), 020503.
- [11] D. Girolami, T. Tufarelli and G. Adesso, "Characterizing Nonclassical Correlations via Local Quantum Uncertainty". *Phys. Rev. Lett.* **110**, 240402 (2013).
- [12] S. Luo, "Wigner-Yanase Skew Information vs. quantum Fisher Information". *Proc. Amer. Math. Soc.* **132**, 885 (2003).
- [13] Adesso G, Datta A, Quantum versus classical correlations in Gaussian states. *Phys. Rev. Lett.* **105**, 030501 (2010).
- [14] K. El Anouz, I. El Aouadi, A. El Allati and T. Mourabit, Dynamics of quantum correlations in quantum teleportation. *Int. J. Mod. Phys. B.* **34**, 10 (2020).
- [15] K. Stannigel, P. Rabl, A.S. Sørensen, P. Zoller, M.D. Lukin, Optomechanical Transducers for Long-Distance Quantum Communication. *Phys. Rev. Lett.* **105**, 220501 (2010).
- [16] O. El Bir, M. El Baz, Quantum correlations under the effect of a thermal environment in a triangular optomechanical cavity. *J. Opt. Soc. Amer. B.* **37**, 11 (2020).
- [17] F. Brennecke, S. Ritter, T. Donner, T. Esslinger, Cavity Optomechanics with a Bose-Einstein Condensate. *Science* **322**, 235 (2008).
- [18] M. Asjad, Quantum degenerate Fermi gas entanglement in optomechanics. *J. Russ. Laser Res.* **34**, 278 (2013).
- [19] H. Mabuchi, A.C. Doherty, Cavity quantum electrodynamics: coherence in context. *Science.* **298**, 1372 (2000).
- [20] H. Mikaeili, A. Dalafi, M. Ghanaatshoar, B. Askari, Ultraslow light realization using an interacting Bose–Einstein condensate trapped in a shallow optical lattice", **12**, 4428 (2022).

- [21] A. Dalafi, M. H. Naderi, A. Motazedifard, Effects of quadratic coupling and squeezed vacuum injection in an optomechanical cavity assisted with a Bose-Einstein condensate, *Phys. Rev. A.* **97**, 043619 (2018).
- [22] M. Ullah, F. Saif, Li-G. Wang, "Four-Wave Mixing Response via Hybrid Coulomb-Coupled Cavity Optomechanics". *Adv. Quan. Tech.* **3**, 8 (2020).
- [23] K-A. Yasir, M. Ayub, F. Saif, "Exponential localization of moving end mirror in optomechanics", *J. Mod. Opt.* **61**, 1318-1323 (2014).
- [24] K. Ullah, H. Jing, F. Saif, "Multiple electromechanically-induced-transparency windows and Fano resonances in hybrid nano-electro-optomechanics". *Phy. Rev. A.* **97**, 3 (2018).
- [25] A. Messikh, M. Wahiddin, C. Pah, Z. Ficek, "The effect of finite bandwidth squeezed light on entanglement creation in the Dicke model", *J. Opt. B: Quantum Semiclassical Opt.* **6**, 289 (2004).
- [26] S. Huang, G. Agarwal, "Entangling nanomechanical oscillators in a ring cavity by feeding squeezed light", *New J. Phys.* **11**, 103044 (2009).
- [27] S. Bougouffa, M. Al-Hmoud, "Bipartite Entanglement in Optomechanical Cavities Driven by Squeezed Light", *Int J. Theor. Phys.* **59**, 1699–1716 (2020).
- [28] G. Adesso, T. Bromley, M. Cianciaruso, "Measures and applications of quantum correlations", *J. Phys. A: Math. Theor.* **49**, 473001 (2016).
- [29] M. Paternostro, S. Gigan, M-S. Kim, F. Blaser, H-R. Böhm, M. Aspelmeyer, "Reconstructing the dynamics of a movable mirror in a detuned optical cavity", *New J. Phys.* **2006**, 8, 107–122.
- [30] M. Asjad, F. Saif, "Steady-state entanglement of a Bose-Einstein condensate and a nanomechanical resonator", *Phy. Rev. A* **84**, 033606 (2011).
- [31] S-L. Braunstein, A-K.Pati, "Quantum Information with Continuous Variables". Springer Science & Business Media, Berlin (2012).
- [32] M-B. Plenio, "Logarithmic negativity: a full entanglement monotone that is not convex", *Phys. Rev. Lett.* **95**, 090503 (2005).
- [33] G. Adesso, A. Serafini, F. Illuminati, "Extremal entanglement and mixedness in continuous variable systems", *Phys. Rev. A.* **70**, 022318 (2004).
- [34] H. Ollivier, W.H. Zurek, "Quantum Discord: A Measure of the Quantumness of Correlations", *Phys. Rev. Lett.* **88**, 017901 (2001).
- [35] X. Yang, G- H. Huang, M- F. Fang, "A study on quantum discord in Gaussian states", *Opt. Comm.* **341**, 91–96 (2015).
- [36] P. Giorda, M. G. A. Paris, "Gaussian Quantum Discord", *Phys. Rev. Lett.* **105**, 020503 (2010).
- [37] M. Gu, H-M. Chrzanowski, S-M. Assad, T. Symul, K. Modi, T-C. Ralph, V. Vedral, P-K. Lam, "Observing the operational significance of discord consumption", *Nat Phys* **8**, 671–675 (2012).
- [38] L-S. Madsen, A. Berni, M. Lassen, U-L. Andersen, "Experimental investigation of the evolution of Gaussian quantum discord in an open system", *Phys. Rev. Lett.* **109**, 030402 (2012).
- [39] S. Groblacher, K. Hammerer, M-R. Vanner, M. Aspelmeyer, "Observation of strong coupling between a micromechanical resonator and an optical cavity field", *Nat.* **460**, 724 (2009).
- [40] A. Schliesser, O. Arcizet, R. Rivière, G. Anetsberger, T-J. Kippenberg, "Resolved-sideband cooling and position measurement of a micromechanical oscillator close to the Heisenberg uncertainty limit". *Nat. Phys.* **5**, 509 (2009).
- [41] A. Fainstein, N-D. Lanzillotti-Kimura, B. Jusserand, B. Perrin, "Strong optical-mechanical coupling in a vertical gaas/alas microcavity for subterahertz phonons and near-infrared light", *Phys. Rev. Lett.* **110**, 3 (2013).
- [42] A. Rueda, W. Hease, S. Barzanjeh, J-M. Fink Electro-optic entanglement source for microwave to telecom quantum state transfer. *npj Quantum Inf.* **5**, 1 (2019).

- [43] P-Y.Hou, Y-Y. Huang, X-X. Yuan, X-Y. Chang, C. Zu, L. He, L-M. Duan, Quantum teleportation from light beams to vibrational states of a macroscopic diamond. *Nat. Commun.* **7**, 11736 (2016).
- [44] P. van Loock, Quantum communication with continuous variables, *Fortsch. Phys.* **50**, PP. 1177-1372 (2002).
- [45] J. Fiurasek , Improving the fidelity of continuous-variable teleportation via local operations. *Phys. Rev. A.* **66**, 012304-18 (2002).
- [46] M-M. Khan, M-J. Akram, M. Paternostro, F. Saif, Engineering single-phonon number states of a mechanical oscillator via photon subtraction, *Phys. Rev. A.* **94**, 063830 (2016).
- [47] K. Hammerer, C. Genes, D. Vitali, P. Tombesi, G. Milburn, C. Simon, D. Bouwmeester, *Nonclassical states of light and mechanics* (Springer, 2014).
- [48] G-O. Heymans, M-B. Pinto, R-O. Ramos, Quantum phase transitions in a bidimensional $O(N) \times \mathbf{Z}$ scalar field model. *J. High Energ. Phys.* **2022**, 28 (2022).
- [49] S-Y. Liu, Y-R. Zhang, W-L. Yang , H. Fan, Global quantum discord and quantum phase transition in XY model. *Ann. Phy.* **362**, 805-813 (2015).
- [50] L-C. Zhao, L. Ling , J-w. Qi, Z-Y. Yang, W-L. Yang, Dynamics of rogue wave excitation pattern on stripe phase backgrounds in a two-component Bose-Einstein condensate. *Comm. Non. Sci. Num. Simu.* **49**, 39-47(2017).